Stacking fault-associated polarised surface-emitted photoluminescence from zincblende InGaN/GaN quantum wells

S. A. Church,[1, a)] B. Ding,[2] P. W. Mitchell,[1] M. J. Kappers,[2] M. Frentrup,[2] G. Kusch,[2] S. M. Fairclough,[2] D. J. Wallis,[2, 3] R. A. Oliver,[2] and D. J. Binks[1]

[1)] *Department of Physics and Astronomy, Photon Science Institute, University of Manchester, Manchester M13 9PL, United Kingdom*

[2)] *Department of Materials Science and Metallurgy, University of Cambridge, 27 Charles Babbage Road, Cambridge CB3 0FS, United Kingdom*

[3)] *Centre for High Frequency Engineering, University of Cardiff, 5 The Parade, Newport Road, Cardiff, CF24 3AA, United Kingdom*

Zincblende InGaN/GaN quantum wells offer a potential improvement to the efficiency of green light emission by removing the strong electric fields present in similar structures. However, a high density of stacking faults may have an impact on the recombination in these systems. In this work, scanning transmission electron microscopy and energy-dispersive x-ray measurements demonstrate that one dimensional nanostructures form due to indium segregation adjacent to stacking faults. In photoluminescence experiments these structures emit visible light which is optically polarised up to 86 % at 10 K and up to 75 % at room temperature. The emission redshifts and broadens as the well width increases from 2 nm to 8 nm. Photoluminescence excitation measurements indicate that carriers are captured by these structures from the rest of the quantum wells and recombine to emit light polarised along the length of these nanostructures.

LEDs based on InGaN/GaN quantum wells (QWs) grown on the c-plane of the wurtzite (wz) crystal structure can have room temperature internal quantum efficiencies (IQEs) up to 90 % for emission in the blue[1]. By increasing the indium content in the QW, the emission wavelength can be extended into the green: however this reduces the IQE, a phenomenon known as the green gap[2]. A significant contribution to this drop in efficiency is the quantum confined Stark effect, which arises due to the strong electric field perpendicular to the QWs. The electric field is a consequence of spontaneous and piezoelectric polarisation effects[3]. A larger indium content increases the strain in the QW and results in an increase in the electric field strength. The electric fields act to separate electrons and holes and thereby reduce the rate of radiative recombination for longer wavelength emitters[4]. An additional contribution to the green gap is that the lower growth temperature required to increase the indium content, lead to a higher density of point defects and an increased rate of non-radiative recombination[5].

The IQE of green QWs thus may be improved by lowering the indium content, to reduce the non-radiative recombination rate. One way to achieve this is to grow QWs on zincblende (zb) GaN, which has a smaller bandgap than wz-GaN by 200 meV[6]. Additionally, zb-GaN has zero spontaneous and piezoelectric fields in the [001] direction[7,8] and therefore the electric field across a QW grown in the (001) plane is zero. Unlike wz-GaN[9], zb-GaN is not birefringent[10], ensuring that the polarisation state of light propagating through it in all directions is preserved.

However, as zb-GaN is thermodynamically metastable during growth, epilayers contain stacking faults (SFs)[11], which have a typical density of $1 \times 10^5\,\mathrm{cm}^{-1}$ at the surface in layers grown so far. These SFs are a change in the stacking order of atoms such that the crystal structure is comparable to wz-GaN in a thin plane[12]. SFs may reduce the IQE of the emission from zb-GaN/AlN QWs at room temperature[13], but the impact of SFs on the emission from zb-InGaN/GaN QWs has yet to be studied.

In this work we present structural and photoluminescence measurements of zb-InGaN/GaN QWs and suggest that the SFs lead to polarised emission at temperatures between 10 K and room temperature. This polarised emission may be useful as a light source for three-dimensional display technologies[14].

The samples were grown on a 3C-SiC/Si (001) substrate, with an offcut of 4° towards the [110] direction, the lattice mismatch with the GaN is 3.4 %[15]. A GaN nucleation layer, with a thickness of 30 nm was initially grown, followed by 500 nm of GaN buffer layer. The GaN was nominally undoped, but secondary ion mass spectroscopy (SIMS) measurements showed that GaN epilayers grown under these conditions had an unintentional oxygen impurity concentration of the order of $1 \times 10^{19}\,\mathrm{cm}^{-3}$. Five InGaN/GaN QWs were subsequently grown using a quasi-two-temperature (Q2T) method[16]; the barriers had a nominal thickness of 16 nm and nominal QW thicknesses of 2 nm, 4 nm, 6 nm and 8 nm were studied. No additional cap layer was included on top of the final GaN barrier.

The structural properties of the QWs were studied by scanning transmission electron microscopy/energy dispersive X-ray (STEM/EDX) using an FEI Tecnai Osiris operating at 200 kV and equipped with four energy dispersive X-ray spectrometers. High-angle annular dark-field (HAADF) images were taken with the beam direction parallel to the [1-10] zone axis. Samples for STEM analysis were prepared using a focussed ion beam (FIB:

[a)] stephen.church@manchester.ac.uk

FEI Helios NanoLab^{TM}) in-situ lift-out method.

The optical properties were investigated with photoluminescence (PL) and PL-excitation (PLE) spectroscopy using a continuous wave HeCd laser at a wavelength of 325 nm, with an excitation power density of 10 W cm^{-2}, and a 300 W Xe lamp coupled to a monochromator with an excitation power density of $\approx$ 0.4 mW cm^{-2} at each wavelength, respectively. The PL was focused onto the slit of a double-grating spectrometer with a spectral resolution of 24 Å. The light was detected using a GaAs photomultiplier tube (PMT) and processed with lock-in amplification techniques. The optical polarisation was analysed with a Glan-Thomson polariser placed at the spectrometer slit, collecting the emission in the [001] direction. The spectral response of the PMT and spectrometer was measured using a calibrated black-body source, and used to correct the PL spectra. A different response was measured for each polariser angle to account for the polarisation response of the grating. PL time decays were obtained by excitation with a 100 fs frequency-tripled pulsed Ti:Sapphire laser with a wavelength of 267 nm resulting in an injected carrier density of 3×10^{12} /cm^2/pulse. Time correlated single photon counting techniques were used to produce PL-decay transients.

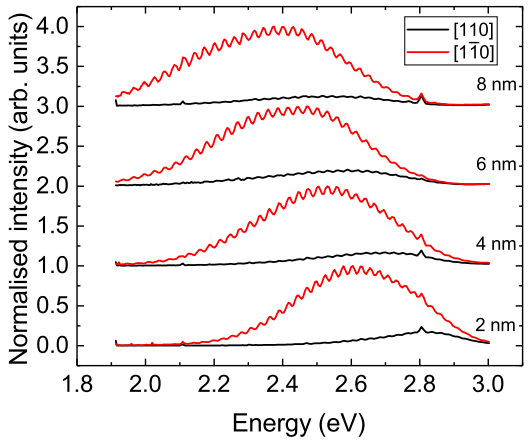

FIG. 1. Room temperature photoluminescence spectra for quantum wells with widths of 2 nm, 4 nm, 6 nm and 8 nm, polarisation resolved in the [110] and [1-10] directions. The spectra have been normalised and offset for each sample for clarity. The peak common to all the spectra at 2.8 eV is a spontaneous emission line from the laser.

The polarised PL spectra at room temperature for each sample are shown in Fig. 1. These spectra exhibit Fabry-Perot interference fringes due to reflections at interfaces[17]. The emission is polarised in [1-10]. This was quantified using the degree of linear polarisation (DOLP), $DOLP = (I_{\max} - I_{\min})/(I_{\max} + I_{\min})$, where $I_{\max,\min}$ are the maximum and minimum integrated intensities of the emission. The DOLP was determined, with an error of $\pm$ 5 %, to be 75 %, 70 %, 65 % and 75 % for QW widths of 2 nm, 4 nm, 6 nm and 8 nm respectively, and is therefore broadly independent of the QW-width.

The emission from the 2 nm sample has a peak energy of 2.62 eV and a FWHM of 420 meV. As the width of the QW is increased to 4 nm, 6 nm and 8 nm, the peak energy of the emission decreases to 2.53 eV, 2.45 eV and 2.38 eV and the FWHM increases to 440 meV, 470 meV, and 510 meV, respectively. The FWHMs of these spectra are large compared with wz-InGaN/GaN MQWs[5,18].

The normalised (X,Y) CIE color values[19] for the PL spectra vary from (0.14, 0.17) for the 2 nm sample to (0.33, 0.51) for the 8 nm sample - which represent the colors blue and yellow-green respectively. This redshift of the emission with increasing QW width is largely compatible with a reduction in the quantum confinement energy at larger QW widths. However, the emission continues to redshift as the QW width increases significantly above the Bohr radius of the electrons and holes (approximately 2.6 nm and 0.26 nm, using dielectric constants and effective masses for zb-GaN[6,20,21]), indicating that another effect is at play.

The high oxygen concentration may lead to a high density of shallow donors in the GaN[22]. This would result in the presence of a high density of free electrons in the QW which would partially fill the conduction band (CB) due to modulation doping effects[23]. The CB filling may be partially responsible for the large FWHM of the emission. Varying the excitation power density by 3 orders of magnitude produced no significant change in the FWHM, consistent with band filling being predominantly due to the high donor density (see Fig S3 in the S.M.).

Carrier localisation is known to strongly influence other InGaN/GaN QW systems[18]. However, the temperature dependent PL, shown in Fig S2 of the S.M., did not show any of the characteristics of such localisation, such as the s-shape peak energy dependence with temperature[24]. However, this does not rule out these effects occurring as they may be obscured by the large FWHM of the two overlapping peaks.

The PL spectra in Fig. 2 indicate that two emission bands are present at a temperature of 10 K, and this is the case for all of the samples studied, as shown in Fig. S1 in the supplementary material (S.M.). For the 2 nm QW, there is a low energy peak centred at 2.67 eV and a high energy peak at 2.86 eV. These energies are higher than the values at room temperature due to the increase in bandgap with decreasing temperature. For the 2 nm QW, the lower energy peak is polarised with a DOLP of 86 % in the [1-10] direction, whereas the high energy peak has a DOLP of 37 %. As the sample temperature is increased, the higher energy peak quenches at a faster rate than the lower energy peak, such that the polarised lower energy peak dominates in the room temperature PL spectra in Fig. 1. This is clearly demonstrated in temperature dependent PL measurements shown in Fig. S2 in the S.M..

To gain a greater understanding of the recombination mechanisms underlying the two emission bands at low

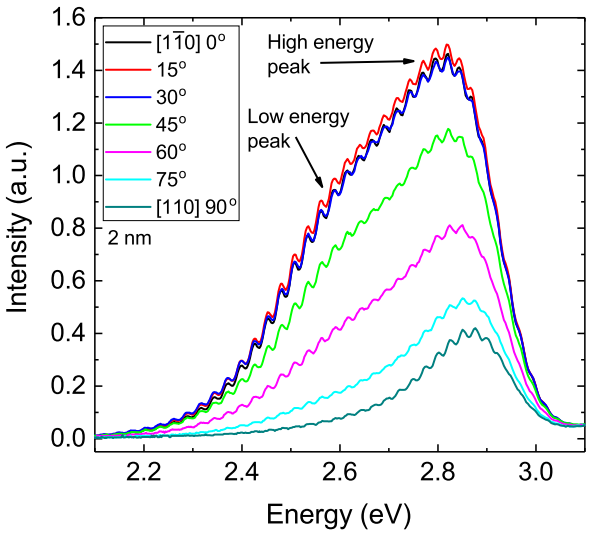

FIG. 2. 10 K polarised PL spectra detecting emission of light polarised at angles between the [110] and [1-10] crystallographic directions for the 2 nm QW.

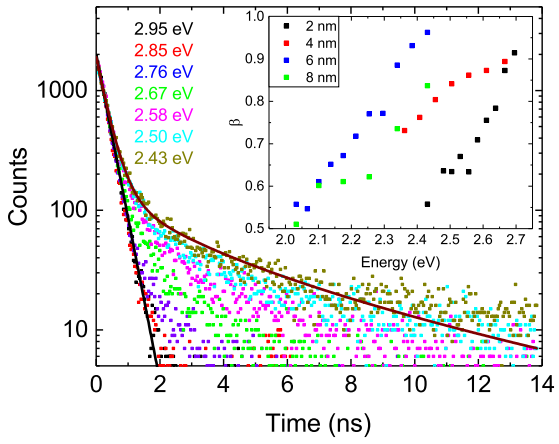

FIG. 3. PL time decays at a temperature of 10 K for the 2 nm QW sample. The lines show the stretched exponential fits to the data at the highest and lowest emission energy studied. The β factor in the stretched exponential fit for different emission energies and QW widths is included in the inset.

temperature, PL time decays were measured at a temperature of 10 K, as shown in Fig. 3. When detecting at an emission energy of 2.95 eV the decays are monoexponential. This decay shape may be a result of the high oxygen concentration[23], which ensures that the electron density, n, is much greater than the hole density, p. n can therefore be considered effectively constant and the rate is only affected by a change in p.

A non-exponential decay component becomes prominent in the spectrum at lower emission energies, which indicates that a different recombination mechanism is responsible for the low energy peak. The non-exponential form may indicate a distribution of different recombination rates with the same emission energy, resulting from recombination of carriers from different local environments.

To investigate the impact of the sample inhomogeneity, and the QW width on the decays, a fit of the form $Ae^{-t/\tau_1} + Be^{-t^\beta/\tau_2}$ was applied to PL decay curves from each sample. The first monoexponential term extracts the lifetime of the high energy mono-exponential decay. The second stretched exponential term applies to the lower energy non-exponential decay and provides an indication of the degree of inhomogeneity by the β term. An example of this fit is shown in Fig. 3, and the variation of β with emission energy for each sample is shown as an inset.

The monoexponential lifetimes were found to be constant with emission energy, with values of 320 ps, 210 ps, 230 ps and 290 ps for increasing QW widths. There is some random variation in the decay time between samples, but no trend as the QW thickness is increased. This may be a consequence of the high density of electrons, which means that the wavefunction overlap with holes, and therefore the rate of radiative recombination, is not strongly dependent on QW width. Any variation in the decay times may be due to disorder in the structures.

The stretched exponential component of the decay function was only required for a good fit to the PL transients for the low energy side of the emission, corresponding to the low energy peak in Fig. 2. The emission energies for which this occurs are reduced for wider QWs due to the redshift of the emission. For all samples, as the emission energy reduces, β reduces, varying between 1.0 and 0.5 depending on the sample. The decays become less exponential at lower energies, indicative of recombination in regions of increased disorder contributing to the lower energy emission. This is qualitatively consistent with the increase in the FWHM for the lower energy emitting samples in Fig. 1.

Structural measurements of the QWs offer an explanation for this lower energy emission. Fig. 4 shows a STEM-EDX map of the 8 nm QW sample. SFs intersect with the QWs on their way to the GaN surface. The EDX measurements show that the indium content within a few nm of the SFs is approximately double the indium content in the rest of the QW. Since the SFs are planar defects, these regions will extend perpendicular to the plane of the image (in the [1-10] direction) resulting in a one-dimensional nanostructure: a quantum-wire. The bandgap of the quantum wire is smaller than in the rest of the QWs and is likely to result in the lower energy peak in the PL spectrum. More detailed examination of the indium content variations in these materials will be published elsewhere[25]. Fig. 4 shows that the QWs have

been grown on a rough zb-GaN surface, which results in a meandering profile when viewed in the [1-10] direction, but not in the [110] direction[11]. This meandering may also result in an additional contribution to the confinement of the carriers in the quantum wires and in the rest of the QW. Anisotropic strain may also contribute to the polarisation of the QW emission[26].

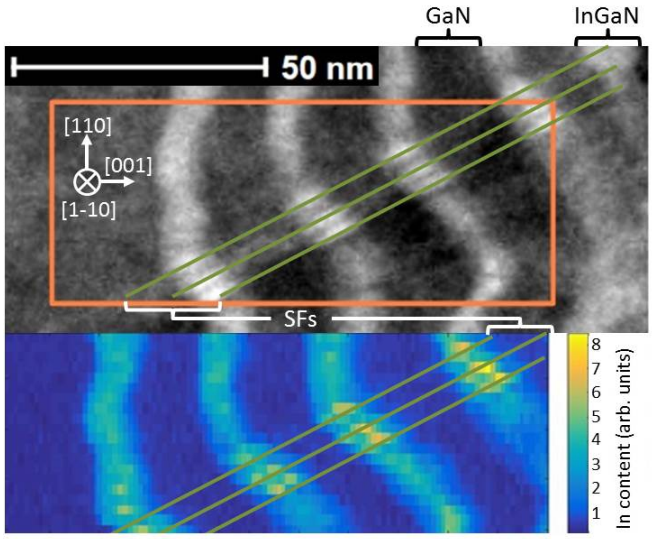

FIG. 4. HAADF STEM image of a 8 nm zincblende InGaN/GaN QW. Included is an EDX relative indium composition map of the intersection between the QWs and SFs.

A PLE spectrum is shown in Fig. 5. When detecting the emission at any wavelength across the PL peak, photon absorption edges can be observed at energies of 3.26 eV and 3 eV. The first absorption edge is at a constant energy and is close to the bandgap of unstrained zb-GaN (3.3 eV[6]). This therefore corresponds to the photogeneration of carriers in the zb-GaN, which are captured by, and recombine in, the QWs. The energy discrepancy suggests that the zb-GaN is under tensile strain, consistent with previous results[27].

The second absorption edge is not at a constant energy. A sigmoidal fit was applied to the PLE spectra to extract characteristic absorption energies across the emission spectrum[28]. When detecting on the higher energy peak, the absorption edge shifts with emission energy, with an energy difference of approximately 250 meV between absorption and emission. This is consistent with direct absorption of photons into QWs, generating electron-hole pairs which cool to the ground states before recombining.

For the lower energy peak, this absorption edge shifts at a reduced rate with emission energy and the absorption edge drops close to zero before the onset of emission. This suggests that there are distinct regions in the QWs with different energy levels: this is consistent with the STEM/EDX measurements in Fig. 4. There will be little direct photon absorption into the quantum wires due to

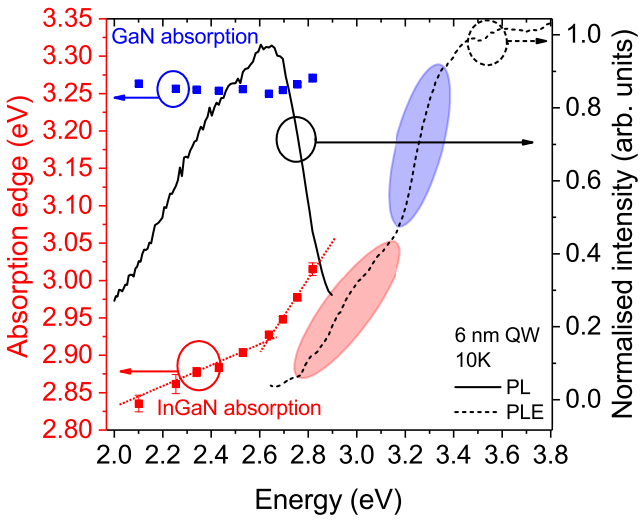

FIG. 5. A PL spectrum at a temperature of 10 K of the 6 nm-thick QW (black), and a PLE spectrum detecting the emission at an emission photon energy of 2.53 eV (black-dashed). The characteristic energies of the GaN (blue) and QW (red) absorption edges extracted from PLE spectra, dotted lines are a guide to the eye to indicate a change in behaviour across the spectrum.

their small volume and low density of states. Instead, carriers are captured from the rest of the QW into the quantum wires: this leads to energy differences up to 800 meV between absorption and emission. As the absorption occurs mainly into unpolarised states, the PL spectra are independent of the polarisation of the excitation source (see Fig. S4 in the S.M.). CB filling may also contribute to this large energy difference by preventing absorption into the filled low energy CB states, whilst the carriers in these filled states can still radiatively recombine.

The large degree of inhomogeneity is a key factor in the recombination from the quantum wires, as evidenced by the large FWHM of the PL spectra in Fig. 1. This may be due to variation in the size and indium content of the quantum wires, and variation in the degree of CB filling. Furthermore, it is thought that the SFs will alter the local electric fields in the structure due to spontaneous polarisation effects[21]. Variation in the SF distribution is therefore another mechanism for increased inhomogeneity in the samples. The fitting of PL decays demonstrates that lower energy recombination originates from regions of greater inhomogeneity, which would correspond to wider quantum wires with more indium content, stronger electric fields and more CB filling.

The optical polarisation of the low energy emission can also be explained by considering recombination in the quantum wires[29]. By changing the cross sectional dimensions of the wire, the DOLP can be changed and it is possible that the DOLP will not vary significantly with

temperature under certain conditions[30]. Simple calculations shown in the S.M. show that it is possible for these conditions to be met in this material system. The high energy emission is also polarised, but to a much lesser extent: this may be a consequence of the meandering shape of the QWs or anisotropic strain in the QWs.

The SFs are present on the {111} planes of zb-GaN[31], which would produce nanostructures along both the [110] and [1-10] directions in the QW. If the distribution of the SFs is uniform on all 4 planes then the net optical polarisation perpendicular to the growth direction will be zero. However, a recent report[11] has shown that the density of SFs is dependent upon the direction of the substrate offcut. This would result in a greater density of SFs in one direction, leading to a net optical polarisation. Additionally, the meandering profile of the QWs is preferentially seen in the [1-10] direction.

In conclusion, optically polarised emission is observed at room temperature from zb-InGaN/GaN QWs, with a DOLP of up to 75 %. This DOLP is similar to those achieved by wz-QWs[26,32–34], but is obtained using standard MOCVD epilayer growth without any further processing steps. The emission can be tuned to cover the visible spectrum with minimal impact upon the efficiency or dynamics of the recombination. The emission is associated with indium-rich quantum wires which form in the QWs due to their intersection with SF defects. The quantum wires capture carriers from the rest of the QWs. At low temperatures the emission from the rest of the QWs can be seen. Further investigations are required to maximise the DOLP by increasing the anisotropy in the SF distribution.

See the supplementary material for low temperature PL spectra of the full QW series, along with the temperature and excitation power dependence of the spectra, demonstrating the lack of evidence for localisation and band filling effects. Low temperature polarised PL and PLE spectra are also included, along with calculations of the carrier ground states in the quantum wires.

This was work funded by EPSRC under grants EP/M010627/1, EP/N01202X/1 and EP/R01146X/1, and Innovate UK under grant 56917-383420. The authors would like to thank Prof. Phil Dawson (University of Manchester) for useful discussions.

DATA AVAILABILITY

Research data supporting this publication are available at DOI: 10.17632/74x2spfrk2.1.

[1]N. Bardsley, S. Bland, L. Hansen, M. Pattison, M. Pattison, K. Stober, and M. Yamada, US Dep. Energy (2015).
[2]M. Auf der Maur, A. Pecchia, G. Penazzi, W. Rodrigues, and A. Di Carlo, Phys. Rev. Lett. **116**, 027401 (2016).
[3]T. Takeuchi, C. Wetzel, S. Yamaguchi, H. Sakai, H. Amano, I. Akasaki, Y. Kaneko, S. Nakagawa, Y. Yamaoka, and N. Yamada, Applied Physics Letters **73**, 1691 (1998).
[4]D. Schiavon, M. Binder, M. Peter, B. Galler, P. Drechsel, and F. Scholz, Phys. Status Solidi B **250**, 283 (2013).
[5]S. Hammersley, M. J. Kappers, F. C.-P. Massabuau, S.-L. Sahonta, P. Dawson, R. A. Oliver, and C. J. Humphreys, Appl. Phys. Lett. **107**, 132106 (2015).
[6]I. Vurgaftman and J. R. Meyer, J. Appl. Phys. **94**, 3675 (2003).
[7]D. J. As, Microelectronics J. **40**, 204 (2009).
[8]S.-H. Park and Y.-T. Lee, Chinese Phys. Lett. **27**, 044208 (2010).
[9]S. Shokhovets, M. Himmerlich, L. Kirste, J. H. Leach, and S. Krischok, Applied Physics Letters **107**, 092104 (2015).
[10]Y. Du, B. Chang, X. Fu, X. Wang, and M. Wang, Optik **123**, 2208 (2012).
[11]L. Y. Lee, M. Frentrup, P. Vacek, M. J. Kappers, D. J. Wallis, and R. A. Oliver, J. Appl. Phys. **125**, 105303 (2019).
[12]A. F. Wright, J. Appl. Phys. **82**, 5259 (1997).
[13]R. M. Kemper, P. Veit, C. Mietze, A. Dempewolf, T. Wecker, F. Bertram, J. Christen, J. K. N. Lindner, and D. J. As, Phys. Status Solidi C **12**, 469 (2015).
[14]J. Geng, Adv. Opt. photonics **4**, 456 (2013).
[15]M. Frentrup, L. Y. Lee, S.-l. Sahonta, M. J. Kappers, F. Massabuau, P. Gupta, R. A. Oliver, C. J. Humphreys, and D. J. Wallis, J. Phys. D. Appl. Phys. **50**, 433002 (2017).
[16]F. Massabuau, N. Piot, M. Frentrup, X. Wang, Q. Avenas, M. Kappers, C. Humphreys, and R. Oliver, Phys. Status Solidi B **1600664** (2017), 10.1002/pssb.201600664.
[17]D. M. Graham, A. Soltani-Vala, P. Dawson, M. J. Godfrey, T. M. Smeeton, J. S. Barnard, M. J. Kappers, C. J. Humphreys, and E. J. Thrush, J. Appl. Phys. **97**, 103508 (2005).
[18]P. Dawson, S. Schulz, R. A. Oliver, M. J. Kappers, and C. J. Humphreys, J. Appl. Phys. **119**, 181505 (2016).
[19]T. Smith and J. Guild, Trans. Opt. Soc. **33**, 73 (1931).
[20]V. Bougrov, M. E. Levinshtein, S. L. Rumyantsev, and A. Zubrilov, *Properties of Advanced Semiconductor Materials GaN, AlN, InN, BN, SiC, SiGe* (John Wiley & Sons, 2001) pp. 1–30.
[21]S. A. Church, S. Hammersley, P. W. Mitchell, M. J. Kappers, L. Y. Lee, F. Massabuau, S. L. Sahonta, M. Frentrup, L. J. Shaw, D. J. Wallis, C. J. Humphreys, R. A. Oliver, D. J. Binks, and P. Dawson, J. Appl. Phys. **123**, 185705 (2018).
[22]R. Niebuhr, K. H. Bachem, U. Kaufmann, M. Maier, C. Merz, B. Santic, P. Schlotter, and H. Jürgensen, J. Electron. Mater. **26**, 1127 (1997).
[23]H. Haratizadeh, B. Monemar, P. P. Paskov, P. O. Holtz, G. Pozina, S. Kamiyama, M. Iwaya, H. Amano, and I. Akasaki, Phys. status solidi **241**, 1124 (2004).
[24]O. Rubel, M. Galluppi, S. D. Baranovskii, K. Volz, L. Geelhaar, H. Riechert, P. Thomas, and W. Stolz, J. Appl. Phys. **98**, 063518 (2005).
[25]B. Ding, M. Frentrup, S. M. Fairclough, M. J. Kappers, A. Kovács, D. J. Wallis, and R. A. Oliver, in preparation (2020).
[26]H. Jönen, H. Bremers, T. Langer, U. Rossow, and A. Hangleiter, Appl. Phys. Lett. **100**, 151905 (2012).
[27]S. A. Church, S. Hammersley, P. W. Mitchell, M. J. Kappers, S. L. Sahonta, M. Frentrup, D. Nilsson, P. J. Ward, L. J. Shaw, D. J. Wallis, C. J. Humphreys, R. A. Oliver, D. J. Binks, and P. Dawson, Phys. Status Solidi B **1600733**, 1600733 (2017).
[28]R. W. Martin, P. G. Middleton, K. P. O'Donnell, and W. Van der Stricht, Appl. Phys. Lett. **74**, 263 (1999).
[29]U. Bockelmann and G. Bastard, Phys. Rev. B **45**, 1688 (1992).
[30]W. H. Zheng, J.-b. Xia, and K. W. Cheah, J. Phys. Condens. Matter **9**, 5105 (1997).
[31]B. Daudin, G. Feuillet, J. Hubner, Y. Samson, F. Widmann, A. Philippe, C. Bru-Chevallier, G. Guillot, E. Bustarret, G. Bentoumi, and A. Deneuville, J. Appl. Phys. **84**, 2295 (1998).
[32]M. Kubota, K. Okamoto, T. Tanaka, and H. Ohta, Appl. Phys. Lett. **92**, 011920 (2008).
[33]S. E. Brinkley, Y.-D. Lin, A. Chakraborty, N. Pfaff, D. Cohen, J. S. Speck, S. Nakamura, and S. P. DenBaars, Appl. Phys. Lett. **98**, 011110 (2011).
[34]S. Marcinkevičius, R. Ivanov, Y. Zhao, S. Nakamura, S. P. DenBaars, and J. S. Speck, Appl. Phys. Lett. **104**, 111113 (2014).